RESEARCH ARTICLES

HGT

Open camera or QR reader and scan code to access this article and other resources online.

Assessment of Pre-Clinical Liver Models Based on Their Ability to Predict the Liver-Tropism of Adeno-Associated Virus Vectors

Adrian Westhaus,[1,2,†] Marti Cabanes-Creus,[1,†] Kimberley L. Dilworth,[1] Erhua Zhu,[3] David Salas Gómez,[4] Renina G. Navarro,[1] Anais K. Amaya,[3] Suzanne Scott,[1,3,5] Magdalena Kwiatek,[6] Alexandra L. McCorkindale,[7] Tara E. Hayman,[7] Silke Frahm,[8] Dany P. Perocheau,[9–11] Bang Manh Tran,[12] Elizabeth Vincan,[12–14] Sharon L. Wong,[15,16] Shafagh A. Waters,[15–17] Georgina E. Riddiough,[12,18] Marcos V. Perini,[18] Laurence O.W. Wilson,[5,19] Julien Baruteau,[9–11] Sebastian Diecke,[8] Gloria González-Aseguinolaza,[4] Giorgia Santilli,[2] Adrian J. Thrasher,[2] Ian E. Alexander,[3,20] and Leszek Lisowski[1,21,22,*]

[1]Translational Vectorology Research Unit, Children's Medical Research Institute, Faculty of Medicine and Health, The University of Sydney, Westmead, Australia; [2]Great Ormond Street Institute of Child Health, University College London, London, United Kingdom; [3]Gene Therapy Research Unit, Children's Medical Research Institute and Sydney Children's Hospitals Network, Faculty of Medicine and Health, The University of Sydney, Westmead, Australia; [4]Gene Therapy and Regulation of Gene Expression Department, IdiSNA, Instituto de Investigación Sanitaria de Navarra, Universidad de Navarra, CIMA, Pamplona, Spain; [5]Australian e-Health Research Centre, Commonwealth Scientific and Industrial Research Organisation, Sydney, Australia; [6]Military Institute of Hygiene and Epidemiology, The Biological Threats Identification and Countermeasure Centre, Puławy, Poland; [7]Inventia Life Science Pty Ltd., Sydney, Australia; [8]Stem Cell Technology Platform, Max Delbrück Centrum for Molecular Medicine, Berlin, Germany; [9]Genetics and Genomic Medicine Department, Great Ormond Street Institute of Child Health, University College London, London, United Kingdom; [10]Metabolic Medicine Department, Great Ormond Street Hospital for Children NHS Foundation Trust, London, United Kingdom; [11]National Institute of Health Research Great Ormond Street Hospital Biomedical Research Centre, London, United Kingdom; [12]Department of Infectious Diseases, Melbourne Medical School, The University of Melbourne at the Peter Doherty Institute for Infection and Immunity, Melbourne, Australia; [13]Victorian Infectious Diseases Reference Laboratory, Royal Melbourne Hospital at the Peter Doherty Institute for Infection and Immunity, Melbourne, Australia; [14]Curtin Medical School, Curtin University, Perth, Australia; [15]Molecular and Integrative Cystic Fibrosis (miCF) Research Centre, University of New South Wales and Sydney Children's Hospital, Sydney, Australia; [16]School of Biomedical Sciences, Faculty of Medicine, University of New South Wales, Sydney, Australia; [17]Department of Respiratory Medicine, Sydney Children's Hospital, Faculty of Medicine, University of New South Wales, Sydney, Australia; [18]Department of Surgery, Austin Health Precinct, The University of Melbourne, Austin Health, Heidelberg, Australia; [19]Applied BioSciences, Faculty of Science and Engineering, Macquarie University, Sydney, Australia; [20]Discipline of Child and Adolescent Health, Faculty of Medicine and Health, The University of Sydney, Sydney, Australia; [21]Vector and Genome Engineering Facility, Children's Medical Research Institute, Faculty of Medicine and Health, The University of Sydney, Westmead, Australia; [22]Laboratory of Molecular Oncology and Innovative Therapies, Military Institute of Medicine, Warszawa, Poland.

[†]These authors' contributed equally to this work.

An earlier draft of this article was posted as a preprint at bioRxiv (doi: content/10.1101/2022.09.28.510021v1).

The liver is a prime target for *in vivo* gene therapies using recombinant adeno-associated viral vectors. Multiple clinical trials have been undertaken for this target in the past 15 years; however, we are still to see market approval of the first liver-targeted adeno-associated virus (AAV)–based gene therapy. Inefficient expression of the therapeutic transgene, vector-induced liver toxicity and capsid, and/or transgene-mediated immune responses reported at high vector doses are the main challenges to date. One of the contributing factors to the insufficient clinical outcomes, despite highly encouraging preclinical data, is the lack of robust, biologically and clinically predictive preclinical models. To this end, this study reports findings of a functional evaluation of 6 AAV vectors in 12 preclinical models of the human liver, with the aim to uncover which combination of models is the most relevant for the identification of AAV capsid variant for safe and efficient transgene delivery to primary human hepatocytes. The results, generated by studies in models ranging from immortalized cells, iPSC-derived and primary hepatocytes, and primary human hepatic organoids to *in vivo* models, increased our understanding of the strengths and weaknesses of each system. This should allow the development of novel gene therapies targeting the human liver.

**Correspondence: Dr. Leszek Lisowski, Vector and Genome Engineering Facility, Children's Medical Research Institute, Faculty of Medicine and Health, The University of Sydney, 214 Hawkesbury Road, Westmead, NSW 2145, Australia. E-mail: llisowski@cmri.org.au*

In the April 2023 issue of *Human Gene Therapy* (vol. 34, no. 7–8; 273–288), the article entitled "Assessment of Pre-Clinical Liver Models Based on Their Ability to Predict the Liver-Tropism of Adeno-Associated Virus Vectors" has been updated on May 2, 2023 after first online publication of April 17,2023 to reflect Open Access, with copyright transferring to the author(s), and a Creative Commons License (CC-BY) added (http://creativecommons.org/licenses/by/4.0).

Keywords: liver gene therapy, AAV, nonhuman primate, xenograft model, hepatocyte

INTRODUCTION

RECOMBINANT ADENO-ASSOCIATED VIRAL (rAAV) vectors are versatile delivery tools composed of a single-stranded DNA genome flanked by 145-bp inverted terminal repeats, packaged within an icosahedral protein capsid. The adeno-associated virus (AAV), from which this vector system was derived, is a nonpathogenic helper-dependent parvovirus with multiple naturally occurring serotypes, including the prototypical serotype 2 (AAV2).[1,2] AAV2 was the first variant to be vectorized and is the best understood serotype, still used in many studies to date.[3,4] The structure and amino acid sequence of the nonenveloped AAV capsid is the main determinant of tropism.[5] Therefore, modifying the viral capsid has been used as a strategy to target specific cell types and organs for therapeutic applications.[6]

Clinical success of gene therapy trials using AAV vectors has led to the authorization of products for three indications to date: RPE65-associated retinal dystrophy (AAV2 capsid; Luxturna™),[7] spinal muscular atrophy (AAV9 capsid; Zolgensma™),[8] and lipoprotein lipase deficiency (AAV1 capsid, Glybera™; no longer available).[9] Although these AAV-based products target different organs (the eye, the central nervous system, or the muscles, respectively), therapies targeting disorders of other organs, such as the liver, have not reached market approval to date.

The liver is an important clinical target for gene therapies because of its key role in metabolism and homeostasis. Most of the experience in liver gene transfer using AAV vectors has been obtained in clinical trials for two coagulation disorders: hemophilia A and B.[10,11] Data from these trials have been encouraging and showed a relatively good safety profile. However, clinical studies conducted to date pointed out several challenges that need to be overcome to facilitate approval of therapeutic products for these diseases and expanding AAVs as therapeutics for other liver disorders. These challenges include the activation of the immune system following vector administration, unexpectedly low efficiency of targeting human hepatocytes *in vivo*, and liver toxicity associated with the administration of high vector doses.[12]

The development of immune responses toward the therapeutic vector, resulting in the reduction of transgene expression, was first observed in a phase I/II study that utilized AAV2 to express Factor IX to treat hemophilia B.[13] AAV2 is endemic to the human population and thus many patients who could benefit from AAV2-based therapeutics have developed immunity to this serotype during their lifetimes, including six of seven patients enrolled in the first systemic clinical AAV2 study. Elevation of liver transaminases and $CD8^+$ T cells against AAV were detected following vector administration through the hepatic artery.[13,14]

Increase in Factor IX levels was only detected in two patients and it was transient, a striking contrast to data obtained in preclinical studies in mice and nonhuman primates (NHPs), which showed long-term transgene expression.[15] Although disappointing overall, the study confirmed the relative safety of rAAV-mediated liver gene transfer.[16] Critically, however, the activation of the immune system was not observed in any of the studies performed in animal models, highlighting the limitations of the model systems used to develop and validate new AAV therapeutics before clinical implementation.

Subsequent liver-targeted trials utilized other serotypes, such as AAV8[17] and AAV5,[18] both selected based on preclinical data in mice and NHPs.[19,20] In a pivotal trial sponsored by St. Jude Children's Research Hospital, a self-complementary AAV8 vector encoding Factor IX was administered to seronegative patients at three different doses.[21] Although long-term clinical efficacy was achieved, an early increase in liver transaminases was observed in the high-dose cohort.[22] Immune adverse events in liver clinical trials can generally be controlled by the administration of corticosteroids to prevent elimination of transduced cells and thus therapeutic transgene expression. Nevertheless, prevalence of neutralizing antibodies (NAbs) reduces the pool of patients that may be able to benefit from novel experimental therapies.

However, clinical studies suggest that anti-AAV5 antibodies do not preclude successful liver transduction with AAV5-based vectors.[23] This vector serotype has also been used to deliver Factor IX at relatively high vector doses (2×10^{13} vector genomes [vg]/kg) with no significant T cell–mediated inflammation,[24,25] although it must be considered that this serotype is also less efficient than others at transducing hepatocytes in animal models.[19]

Despite these current limitations, it remains clear that vector serotype selection plays a crucial role in obtaining the desired clinical outcomes. AAV serotypes used in clinical studies are selected based on data generated in preclinical, frequently murine, models. However, clinical data obtained with AAV2, AAV5, and AAV8 clearly indicate that AAV liver tropism, which can be species specific,[20] can differ significantly between the murine or NHP preclinical models and human patients.[11]

One way to overcome this issue has been using ''humanized'' models to functionally evaluate the existing AAV variants for their ability to transduce human hepatocytes *in vivo*. The same models can also be used to identify novel capsids with improved liver tropism. To this end, bioengineered capsids with high tropism toward human hepatocytes, such as AAV-LK03[26] and AAV-NP59,[27] were developed in xenografted *Fah*$^{-/-}$/*Rag2*$^{-/-}$/*Il2rg*$^{-/-}$ (FRG)[28] mice demonstrating the validity of this

approach. The shuffled capsid AAV-LK03, bearing high sequence similarity to the natural serotype AAV3b,[1,29] has been the first non-natural AAV to be used in clinical studies and led to stable therapeutic levels of Factor VIII expression in 16 of 18 hemophilia A patients.[30]

Two patients treated at the highest dose in this study lost Factor VIII expression likely as a result of immune activation against the vector.[30] AAV-NP59, a highly functional variant selected in humanized FRG (hFRG), which differs from prototypical AAV2 at 11 amino acids only,[31] is yet to be tested in the clinic. Another interesting approach was recently published by the Asokan laboratory in the area of AAV capsid engineering for the central nervous system.[32] In this study, a cross-species compatible capsid was engineered by directed evolution in pigs, mice, and NHPs. The resulting capsid offers cross-species functionality as a result of the successive selection rounds that were performed in the three animal species.

The clinical progress is further affected by our inability to directly compare clinical data obtained from liver gene transfer studies using different AAV vectors not only owing to the differences imposed by the individual AAV variants used, but also owing to the lack of consistency regarding preclinical models used. Furthermore, vector manufacturing protocols, quantification methods, and transgene expression cassettes differ between the individual studies conducted to date.[33] Finally, patient-to-patient variability adds yet another level of complexity and ''noise'' in clinical data, making it very difficult to draw conclusions on how individual vector performance compares with one another.

The choice of the therapeutic cassette is dictated by the specific indication being targeted, and the patient-to-patient differences are impossible to overcome. However, the lack of consistency in the preclinical models used to select the rAAV variant needs to be addressed to determine critical decisions such as selection of the vector type and clinical vector dose. Advances in this respect will enable the successful development of novel effective and safe gene therapeutics.

With this in mind, we set out to compare AAV-based gene transfer efficiency targeting the liver in 12 frequently used preclinical models, including *in vitro* models, such as hepatic cell lines, human-induced pluripotent stem cell (hiPSC)–derived hepatocytes (iHeps), and adult stem cell–derived hepatic organoids. However, the focus was on *ex vivo* models, such as 2D and 3D primary NHP and human hepatocytes cultures, and *in vivo* models, including murine and human hepatocytes in xenograft mice and NHPs. To ensure the data obtained were not unique to the specific AAV variant used in the study, we performed the studies using six natural and bioengineered AAV variants, including four that have previously been utilized in liver-directed clinical studies.

Moreover, to increase quality and impact of the study by minimizing experimental noise, we used a well-characterized barcode approach, which allowed us to compare the individual vectors at the cell entry and transgene expression levels in parallel using next-generation sequencing (NGS) in each of the models.[34–36] This study was aimed to understand the differences between the models and what will be required to address future preclinical translation. On top of the expected differences between the models in respect to their serological and immunological properties, we identified surprising differences between NHP and human hepatocytes that might explain some of lower-than-expected outcomes of clinical trials to date.

MATERIALS AND METHODS

Cell culture conditions and cell origins

AAV production and anti-AAV neutralization assays were performed in a human embryonic kidney (HEK) 293T cell line (Cat. No. CRL-3216; ATCC). HEK293T cells were cultured in Dulbecco's modified Eagle's medium (DMEM; Cat. No. 11965; Gibco) supplemented with 10% fetal bovine serum (FBS; Cat. No. F9423; Sigma-Aldrich), 1×Pen Strep (Cat. No. 15070; Gibco), and 25 mM HEPES (Cat. No. 15630; Gibco). Human hepatocellular carcinoma 7 (HuH-7) and hepatocellular carcinoma HepG2 cells were provided by Dr Jerome Laurence (The University of Sydney) and Prof. Ian E. Alexander, respectively, and cultured in DMEM supplemented with 10% FBS, 1×Pen Step, and 1×nonessential amino acids (Cat. No. 11140; Gibco).

Cell transductions

Transductions were performed as previously published.[36,37] In brief, AAVs were added the indicated amount of rAAV capsid or vector mix to the cells, changing media after 6–8 h and harvesting cells for DNA/RNA or flow cytometry processing 72 h after rAAV exposure, unless otherwise specified.

Origin and culture of iHEP

Frozen iHeps (from ChiPSC18) were purchased at Takara Bio Europe AB, thawed, plated, and maintained according to the manufacturer's instructions in media included in the kit (Cat. No. Y10134; Cellartis Enhanced hiPS-HEP v2). In brief, 8.2×10^5 cells per well were thawed and seeded in a 24-well plate, exposed to AAVs after 5 days in culture, and harvested 7 days after exposure.

Primary human hepatocytes in 2D and 3D culture

Human (HUM4198; Lonza) and rhesus macaque (Cat. No. MKR103; Lonza) primary hepatocytes were used for 2D and 3D culture systems. For 2D culture, 24-well plates were coated with collagen for 45 min. After washing the coated wells with phosphate-buffered saline, primary he-

patocytes were seeded 400,000 cells/well in complete hepatocyte plating media (HCM kit; Cat. No. CC-3198; Lonza). After 4 h of incubation at 37°C and 5% CO_2, media were removed and gently covered with hepatocyte maintaining media (HCM kit; Cat. No. CC-3198; Lonza) containing 0.25 mg/mL Matrigel (Cat. No. 354234; Corning) and incubated at 37°C for 90 min. The AAV mix was added diluted in hepatocyte basal media (HBM; Cat. No. CC-3199; Lonza). Media were changed daily for 3 days, until harvest using Cell Recovery Solution (Cat. No. 354253; BD) and processing for NGS.

The 3D printed hydrogels containing human and rhesus hepatocytes were generated using a Rastrum Cell Printer (Inventia, Sydney, Australia). The cell printing followed the manufacturer's instructions and previously published protocols.[38,39] In brief, hepatocytes were thawed, resuspended in crosslinker solution (Inventia), and printed in 96-well plates at 8,000 cells/well. Cells were maintained in HBM and AAVs were added as described previously. Cells were harvested as whole printed gels and processed for NGS.

Primary human and simian hepatocytes engrafted into FRG mice

Cynomolgus and rhesus macaque primary hepatocytes were purchased from Lonza (Cat. No. MKC118 and Cat. No. MKR103). Human hepatocytes were also purchased from Lonza (Cat. No. HUM181971) and corresponded to a 15-month-old donor.

The engraftment procedure was performed as previously published.[28,40] Mouse studies were supported by the BioResources Core Facility at Children's Medical Research Institute. All animal care and experimental procedures were approved by the joint Children's Medical Research Institute and The Children's Hospital at Westmead Animal Care and Ethics Committee. The FRG mice were housed, treated, and killed following previously published methods.[40]

Liver organoid transduction

Human liver organoids were generated as previously described[41] and used for research purposes with approval from the human ethics committee of School of Biosciences, University of Melbourne (Ethics No. 1851272). To carry out transduction with AAV, the Matrigel-supported planar infection method was adapted.[42] In brief, mature liver organoids embedded in Matrigel domes were isolated by dispersing Matrigel with cold basal media. After centrifugation, the medium was discarded, and the organoid pellet was suspended with expansion medium containing 10 μM Y-27632 (Cat. No. S1049; Selleckchem). The AAV cocktail was added to the medium at the described dose, and then the organoid–AAV mixture was transferred to a 24-well plate precoated with 80 μL of 75% Matrigel.

The organoid–AAV mixtures were incubated at 37°C with 5% CO_2 for 12 h in a planar manner after which organoids on the Matrigel surface were collected, transferred to a tube, centrifuged, and supernatant discarded. The organoids were then washed with cold basal media followed by centrifugation. After the final wash and centrifugation, the organoids were returned to 3D culture by resuspending in Matrigel and seeding at 50 μL per well into 24-well plates. Once the Matrigel had set, 450 μL of expansion culture medium (Supplementary Table S1) was added and then replaced every other day for 7 days. To harvest, the organoids were suspended in cold basal media after the medium was discarded, pelleted by centrifugation, and then snap frozen until processing for DNA and RNA extraction. All centrifugations were carried out at 400 *g* at 4°C for 5 min.

Polymerase chain reaction

Standard and Illumina amplicon-seq NGS polymerase chain reactions (PCRs) were performed using Q5 (Cat. No. M0491; NEB), dNTPs (Cat. No. N0447; NEB), and primers (all Sigma-Aldrich; Supplementary Table S2) and were performed strictly following previously published protocols.[36]

AAV production

All AAV capsids used in this study were produced using polyethylenimine transfection of the LSP-GFP-barcode (LSP-BC) transgene cassette,[31,37,43,44] as well as adenovirus and Rep2-Cap2/3/5/8/LK03/NP59 helper plasmids using previously described methods.[37] The resulting cell lysates and purified media were either purified using iodixanol gradients (all experiments apart from NHP) or CsCl ultracentrifugation (for NHP vectors) following the previously published protocols, respectively.[26,36] AAV titers were established using quantitative PCR and enhanced green fluorescent protein (eGFP) primers following previously published methods.[36,45] The capsids were then mixed at an equimolar ratio as previously described.[36]

Neutralization assays

For experiments using the NHP, neutralization assays determining the anti-capsid antibodies for the different AAVs for all indicated timepoints were performed after the following protocol. At day 1, HEK293T cells were seeded into a 96-well plate at a density of 10^4 cells/well. At day 2, NHP sera were diluted in DMEM supplemented with 2% FBS in a total volume of 100 μL, beginning with a 1:5 dilution followed by dilution series of 1:3 and mixed with a dose of 10^4 vg/cell of the corresponding AAV serotype coding for luciferase that were incubated for 2 h at 37°C. The mix was subsequently used to transduce target cells. Each serum dilution was tested in duplicate.

Negative controls of nontransduced cells, as well as positive controls of cells transduced without AAVs not

preincubated with NHP serum were included in each plate. The transduced cells were incubated for 48 h before quantification of luciferase activity was performed. Light emission from each well was measured in photons/s. The NAb titer was calculated using the highest dilution for which the percentage of light emission was 50% of positive control without serum. A 1:5 dilution of serum reducing the vector transduction by 50% or more was considered positive. The highest positive serum dilution determined the NAb titer.

For antibody determination in human serum samples, the assay was performed as previously described.[46] In brief, HuH-7 cells were incubated with heat-inactivated sera at dilution starting from 1:5, continuing in twofold serial dilutions to 1:1,280. The diluted serum samples were incubated for 1 h at 37°C with the individual AAV capsids diluted in an equal volume of DMEM. rAAV vectors were incubated at the same concentration to reach a predetermined final variant-dependent dose into a 100 μL final volume for transduction. The appropriate dose used was 6,000 vg/cell for AAV2, 2,000 vg/cell for AAV3, 40,000 vg/cell for AAV5, 25,000 vg/cell for AAV8, 2,000 vg/cell for AAV-LK03, and 4,000 vg/cell for AAV-NP59. Pooled human serum samples were used as a positive control.

Quantification of GFP-positive cells was performed by mean fluorescence using flow cytometry 72 h after rAAV exposure. A 1:5 dilution of serum reducing the vector transduction by 50% or more was considered positive. The highest positive serum dilution determined the NAb titer.

Human serum samples

Human serum samples from the Immunology laboratory, Great Ormond Street Hospital for Children NHS Foundation Trust, London, United Kingdom were anonymously analyzed following the guidelines of the Royal College of Pathologists.

NHP work

Animal procedures were approved by the ethical committee for animal testing of the University of Navarra and by the Department of Health of the government of Navarra (Comité de Etica para la Experimentación Animal code: 038/15) and performed according to the guidelines from the institutional ethics commission. Animal welfare checks were performed by animal care staff twice daily.

One young adult male *Macaca fascicularis* NHP was tested negative for anti-AAV NAbs for AAV2, AAV5, and AAV-LK03 and with low seropositivity against AAV3, AAV8, and AAV-NP59.

On day 0, the NHP was anesthetized, blood was drawn to obtain serum, and the animal was subjected to the immunoadsorption process (described in Salas et al.[47]). Within the following 30 min after immunoadsorption, the vector was infused via the saphenous vein over 10 min. Blood was collected at 1 h, 24 h, and 7 days after administration of the vector. At day 7, the animal was killed, and different organs and tissues were collected for further analysis.

DNA and RNA extraction from cells and tissue samples

DNA and RNA were isolated from the cell pellets from the *in vitro* and *ex vivo* experiments using the AllPrep DNA/RNA Mini Kit (Cat. No. 80204; QIAGEN) following the manufacturer's instructions.

DNA from the mouse, NHP, and human hepatocytes from xenograft FRG mice and NHP tissues were isolated using phenol–chloroform extraction after proteinase K digestion following previously published protocols.[36] RNA from the mouse, NHP, and human hepatocytes from xenograft FRG mice and NHP tissues was extracted using the TriReagent (Cat. No. T9424; Sigma)–chloroform protocol previously published.[36,37]

Reverse transcription of extracted RNA

Clean-up of extracted RNA was performed using TURBO DNase (Cat. No. AM1907; Invitrogen) twice for 1 h, followed by incubation with DNAse inactivation reagent following the manufacturer's instructions. The DNase-treated RNA was then used for cDNA synthesis using the SuperScript IV First-Strand Synthesis System (Cat. No. 18091050; Invitrogen) following the manufacturer's instructions using 2 μM of WPRE-binding primer (WPRE_R; Supplementary Table S2) to specifically synthesize the barcoded ssAAV-LSP-GFP-BC-WPRE cDNA.

Next-generation sequencing

The NGS amplicons were prepared and analyzed as previously published.[36,37]

Normalization of NGS reads

NGS data obtained from all samples were normalized to the barcode contribution of the respective input (as indicated previously). Read counts for each sample and each variant were multiplied by the variant-specific ''normalization coefficient'' of the respective input, which was calculated as follows:

$$Normalization\ coefficient = \frac{\%\ of\ NGS\ reads^{expected}}{\%\ of\ NGS\ reads^{measured}}.$$

RESULTS AND DISCUSSION

Study design

To compare the performance of different AAV variants in preclinical models of the human liver, we created an equimolar mix of the following six AAV variants: AAV2, AAV3b, AAV5, AAV8, AAV-LK03, and AAV-NP59;

encoding barcoded expression cassettes compatible with NGS-based readout at the cell entry (DNA) and transgene expression (RNA/cDNA) levels.[31,36,43] AAV2, AAV5, AAV8, and the bioengineered AAV-LK03 chosen as clinical data from liver-targeted human studies was publicly available.[11] AAV-NP59 and AAV3b were included because they were the bioengineered variant of AAV2 and the closest natural relative of AAV-LK03, respectively (Supplementary Fig. S1).

The mix of the six AAV candidates was used to transduce all different preclinical models evaluated in this study, whereas the individual AAV candidates underwent seroprevalence studies using individual human sera. The functional data obtained were compared with publicly available data on AAV performance in clinical trials as well as between the models to identify differences (Supplementary Fig. S1).

In vitro and *ex vivo* models of the human liver

The simplest models of human hepatocytes are based on cell lines derived from hepatocellular carcinoma, such as HuH-7, or hepatocellular blastoma, such as HepG2 cells.[48,49] These lines are immortalized and self-renewing, allowing for low-cost high-throughput experimentation using standard laboratory equipment and reagents. To evaluate both cell types for their potential to serve as biologically predictive models of human primary hepatocyte transduction, cells were transduced at a dose of 1,000 and 200 vg/cell and were harvested 72 h after AAV exposure.

Cell pellets were processed for DNA and RNA/cDNA, which allowed us to evaluate relative vector performance at the cell entry and transgene expression levels, respectively (Supplementary Fig. S2). The NGS results showed that AAV2 outperformed the other variants at the DNA and RNA levels in both HuH-7 and HepG2 cells. Of interest, whereas AAV-LK03 and AAV3b performed similarly at the cell entry level (DNA) in HuH-7 cells, AAV-LK03 outperformed AAV3b at the transgene expression level (RNA). In HepG2 cells, AAV-LK03 and AAV3b performed similarly but were less efficient at both DNA and RNA/cDNA levels than AAV5. The strong performance for AAV2 in those cell lines was expected based on data from HuH-7 cells we reported previously.[36]

Next, we studied the six vectors in iHeps and adult stem cell–derived ductal organoids. It quickly became apparent that the transcriptional dominance of AAV2, as shown in the immortalized cell lines, did not fully translate to iHeps. AAV2 was still able to enter the cells at the highest efficiency at the DNA level, followed by AAV-LK03, AAV3b, AAV5, AAV-NP59, and AAV8 (Fig. 1b), but at the transgene expression level, AAV-LK03 outperformed all other vectors (Fig. 1c).

Using adult stem cell–derived ductal organoids consisting of liver ductal progenitor cells,[50] we found AAV5

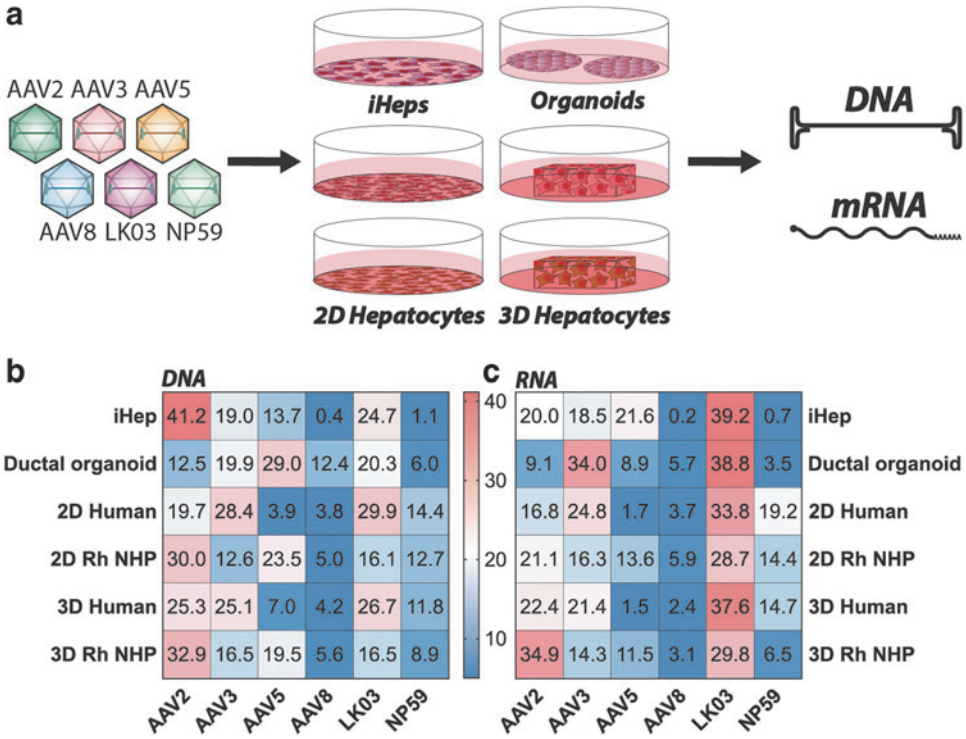

Figure 1. *Ex vivo* results in human and NHP liver models. **(a)** Schematic of transduction of indicated *in vitro* and *ex vivo* models. **(b)** NGS read contribution (%) for each AAV from extracted DNA. **(c)** NGS read contribution (%) for each AAV from mRNA-derived complementary DNA. AAV, adeno-associated virus; NGS, next-generation sequencing; NHP, nonhuman primate.

to be most effective at entering cells (29% of NGS reads at the DNA level) (Fig. 1b). However, the efficient entry of AAV5 did not lead to efficient transgene expression, where only 8.9% of the NGS reads from RNA/cDNA could be attributed to this variant. Instead, AAV-LK03 (38.8%) and AAV3b (34%) were most efficient at transgene expression in the organoids (Fig. 1c), despite less efficient entry (20.3% and 19.9% DNA NSG reads for AAV-LK03 and AAV3b, respectively). The observed decrease in the performance of AAV2 might indicate reduced importance of binding to heparan sulfate proteoglycan (HSPG) as a critical step for cell entry.[43]

To understand how the previous findings translate to primary cells *ex vivo*, human and rhesus monkey (*Macaca mulatta*) hepatocytes were seeded in 2D culture as well as 3D-printed in a hydrogel.[51] The 2D cultured hepatocytes from human and NHP were exposed to three different AAV doses (1,000, 500, and 200 vg/cell) and harvested 3 days after exposure to AAV. The hepatocytes of human origin were most efficiently entered by AAV-LK03 and AAV3b, followed by AAV2, AAV-NP59, AAV5, and AAV8 (Fig. 1b). In contrast, rhesus monkey primary hepatocytes were most efficiently entered by AAV2, followed by AAV5, AAV-LK03, AAV-NP59, AAV3b, and AAV8 (Fig. 1b), showing a marked difference compared with transduction observed in the human hepatocytes.

However, at the level of transgene expression, AAV-LK03 was the most efficient variant in both species. In human hepatocytes, it was followed by AAV3b, AAV-NP59, AAV2, AAV8, and AAV5, whereas in simian hepatocytes it was followed by AAV2, AAV3b, AAV-NP59, AAV5, and AAV8 (Fig. 1c).

As the next step, we wanted to transduce the same cells, but 3D printed in a hydrogel substrate.[38] However, before doing so, we evaluate the potential effect of the 3D culturing system on primary hepatocytes by performing RNAseq using cells before and after 3D culture (Supplementary Fig. S3). The results showed that although expression of most genes did not change substantially, several genes underwent upregulation and downregulation after 3 days of the 3D culture (Supplementary Fig. S3b and Supplementary Table S3). For the human hepatocytes, the most upregulated gene was a long noncoding RNA (PCAT1) with the proposed function of regulating genes implicated in increased cell proliferation, migration, and invasion.[52,53] Owing to a lack of comprehensive annotation coverage of the rhesus monkey genome, the RNAseq data recovered for this species was less informative than the human data.

Hepatocytes in 3D hydrogel cultures were exposed to a dose of 500 vg/cell and cells were harvested and processed for analysis 3 days later. Results obtained showed number of differences compared with results obtained with conventional 2D cultures. Consistent with the 2D cultures, AAV-LK03 entered 3D-printed human hepatocytes with the highest efficiency among the vectors tested but was more closely followed by AAV2 and AAV3b. AAV-NP59, AAV5, and AAV8 performing substantially less efficiently. In the 3D-printed simian hepatocytes, AAV2 was found to be the most effective variant at cell entry, followed by AAV5, AAV3b, and AAV-LK03, with AAV-NP59 and AAV8 being the weakest performers (Fig. 1b). At the transgene expression level (RNA), AAV2 gained in function in both human and rhesus cells compared with 2D cultures.

The data from 2D versus 3D culture systems as well as human versus NHP hepatocytes led to interesting observations. Although AAV2 worked in 2D and 3D cultures of both species, there was a substantial increase in AAV2 performance in the 3D culture system over the 2D culture. This observation could be explained with strong reliance on HSPGs in the 3D-printed hepatocytes, a question we explored further in subsequent studies. Furthermore, the data showed that AAV5 had a markedly higher performance in NHP-cultured hepatocytes than in human hepatocytes, which might explain why clinical trials using AAV5 need very high vector doses and have a lower efficacy than NHP data would suggest.[24,25]

Another upregulated gene that is potentially relevant for AAV biology was glypican proteoglycan 6, a cell surface protein known to harbor HSPGs.[54] This could explain the increased transduction by AAV2 and decreased transduction by AAV-NP59, which has lower affinity to HSPG (Fig. 1),[31] in the 3D printed human hepatocytes compared with the conventionally cultured human hepatocytes.

In summary, in the simplest models of human hepatocytes, the immortalized cancer cell lines, AAV2 performed substantially better than all other variants tested. This performance decreased in stem cell–derived models and primary cells, where the performance of the bioengineered variant AAV-LK03 improved in both human and simian cells. The bioengineered AAV-NP59 also seemed to have improved in primary cells of human origin compared with its performance in immortalized cells and stem cell–derived models. One of the most interesting observations was the relatively variable performance of AAV5 across the models tested. The performance was low in HuH-7 cells and primary human hepatocytes, whereas a relatively high performance was observed in HepG2 cells, stem cell–derived iHeps, and ductal organoids, as well as primary NHP hepatocytes. This might indicate that AAV5 (the most distantly related AAV capsid of the ones chosen for this study) might utilize distinct cell entry and transduction mechanism.

Xenograft *in vivo* models of human and NHPs livers

Having studied the six vectors in several *in vitro* and *ex vivo* models, we next wanted to evaluate one of the com-

monly used *in vivo* xenograft model of the human liver, namely the FRG mouse.[28] To facilitate the comparison with the data obtained from the *ex vivo* studies, we used primary human hepatocytes and primary rhesus hepatocytes, same as in the 2D and 3D culture studies, to engraft livers of female FRG mice. In addition, with the aim to increase the impact of the study, we included primary hepatocytes from the cynomolgus monkey (*M. fascicularis*). The use of a xenograft model, engrafted with either human or NHP hepatocytes, enabled a side-by-side comparison of vector tropism in murine and human or NHP cells *in vivo*.

Thus, we generated hFRG and two types of ''simianized'' FRG, RhFRG, and CyFRG, based on rhesus and cynomolgus origin of cells, respectively. Animals were allowed to repopulate to a replacement index ranging from 15% to 70% and were subsequently systemically injected with the equimolar mix of the six barcoded AAV vectors (Fig. 2a). Livers were harvested 7 days after transduction. Analysis of vector function at the DNA (cell entry) level was performed in sorted GFP$^+$ and unsorted (total ''bulk'' fraction) human and simian cells, whereas analysis at the RNA level (transgene expression) was only performed on human and simian cells sorted based on the vector-encoded GFP marker (GFP$^+$).

At the cell entry level, AAV-NP59 was the most effective variant in all three xenograft models irrespective of analysis being performed on GFP$^+$-sorted or bulk cells (Fig. 2b, c). In bulk human cells, AAV-NP59 was followed by AAV-LK03/AAV3b, AAV2, and AAV8, with AAV5 being the weakest performer. The order of vectors based on cell entry efficiency was overall similar in GFP$^+$ human cells, with the exception that the relative contribution of AAV2 decreased substantially, suggesting that AAV2 transduced human cells but was less efficient at driving transgene expression. We also observed a relative drop for AAV3b and a corresponding increase in signal for AAV-NP59 (Fig. 2c).

Looking at functional transduction (RNA/cDNA) of human hepatocytes in the FRG model, AAV-NP59 performed best in GFP$^+$ human hepatocytes, with AAV-LK03, AAV3b/AAV8, AAV2, and AAV5 following behind.

The results for vector entry into macaque hepatocytes engrafted in FRG mice (RhFRG and CyFRG) were very similar to those obtained in humanized mice with AAV-NP59 being the serotype most efficient at cell entry (Fig. 2b). However, in bulk macaque hepatocytes, AAV-NP59 was followed by AAV8 (instead of AAV-LK03), AAV2 (instead of AAV3b), AAV-LK03, AAV3b, and AAV5 (Fig. 2b). When analyzing GFP$^+$ cells, we observed that highly performing variants AAV-NP59, AAV8, and AAV-LK03 showed an overall gain in contribution at the entry level, performance of AAV3b did not change substantially, whereas AAV2 and AAV5 showed a drop in efficiency compared with unsorted cells (Fig. 2c). Data from analyzed RNA confirmed this trend with AAV-NP59 showing by far the strongest contribution in simian cells sorted for GFP expression. AAV8 was the second-best performing variant and AAV-LK03, AAV3b, AAV2, and AAV5 variants had lower contributions at the transcriptional level (Fig. 2d).

Expectedly, this experiment indicated that the analysis of vector performance at the DNA level using cells sorted for transgene expression (GFP$^+$) is more closely aligned with the analysis at the RNA level than when analyzing DNA from bulk human/NHP hepatocytes. However, bulk DNA data are useful to gain insight into the cell–vector

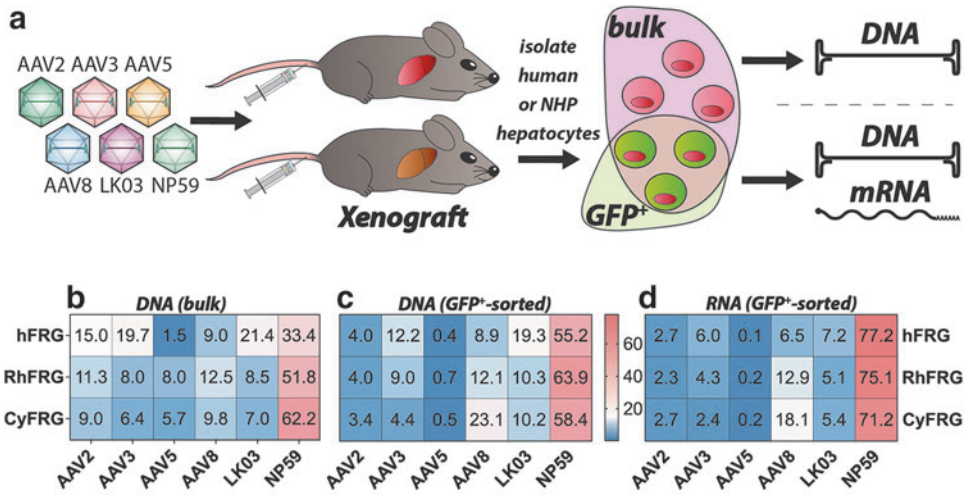

Figure 2. NHP and human xenograft *in vivo* results. **(a)** Schematic of transduction of engrafted FRG mice. **(b)** NGS read contribution (%) for each AAV from extracted xenograft bulk DNA. Cells were sorted for xenograft species only. **(c)** NGS read contribution (%) for each AAV from extracted eGFP-positive xenograft hepatocyte DNA. Cells were sorted for xenograft species as well as eGFP expression where indicated. **(d)** NGS read contribution (%) for each AAV from xenograft mRNA-derived complementary DNA. Cells were sorted for xenograft species as well as eGFP. eGFP, enhanced green fluorescent protein; FRG, *Fah*$^{-/-}$/*Rag2*$^{-/-}$/*Il2rg*$^{-/-}$.

interactions that are not leading to strong transgene expression. The analysis at the DNA level revealed that xenograft models show the same trend regarding AAV5's performance in human and NHP hepatocytes. The *in vivo* xenograft data indicated that AAV5 interacts with, or enters, NHP hepatocytes relatively well but encounters some intracellular block, preventing it from efficiently completing all necessary steps that lead to transgene expression.

The high performance of AAV-NP59 in hFRGs was expected based on previously generated data that showed a strong advantage over the five other AAVs used in this study.[36] The fact that we see a similar trend for the NHP-repopulated FRG mice was a very interesting finding, which may indicate a high performance of this variant in human/primate hepatocytes or a particularly xenograft-specific high performance.

NHP *in vivo* transduction

In the next part of the study, we compared the performance of the six vectors *in vivo* in a widely accepted preclinical model of human liver, the NHP (Fig. 3a). To enable studies of multiple vectors in the same immunocompetent animal, the cynomolgus monkey underwent immunoadsorption (antibody depletion) to reduce antibody concentration, as previously described.[47] Following this treatment, the NHP was infused with 4.2×10^{13} vg total (1.3×10^{13} vg/kg; 7.0×10^{12} vg/variant) of the barcoded AAV mix. The animal was killed 1 week after systemic vector infusion and 21 different tissues were harvested and processed for downstream analysis.

The samples were analyzed for vector copy number using droplet digital polymerase chain reaction (ddPCR) and transgene expression using reverse-transcriptase-ddPCR (Supplementary Table S2; Fig. 4b). As the liver was the main organ of interest in this study, samples were taken from eight different regions of the liver (see Supplementary Fig. S4a for indication of the liver regions analyzed) as well as from the gallbladder and the liver capsule and were analyzed for individual vector performance at the cell entry (DNA) and transgene expression (RNA/cDNA) levels using NGS. As expected based on previous publications,[36,55] and the fact that all six vectors studied are known to be liver tropic, vector copy number analysis showed that at the dose used the liver, gallbladder, and spleen were the organs with the highest levels of transduction (Supplementary Fig. S4b).

Nonliver organs appeared to be most efficiently entered by AAV5 (Supplementary Fig. S4c). Whether these results are truly reflecting the ubiquitous activity of AAV5 or are an artifact of the very low vector copy number in these organs cannot be inferred from this dataset. Unsurprisingly, given that the GFP transgene expression was driven by the ApoE/hAAT liver-restrictive promoter, transgene expression could only be detected in the liver and gallbladder (Supplementary Fig. S4b).[37,56,57]

With the caveat that data were obtained from a single NHP, NGS analysis of liver samples showed that AAV-LK03 and AAV3b were the most effective variants at transducing most regions of the liver. AAV-NP59 was the next best performer, followed closely by AAV5. Of inter-

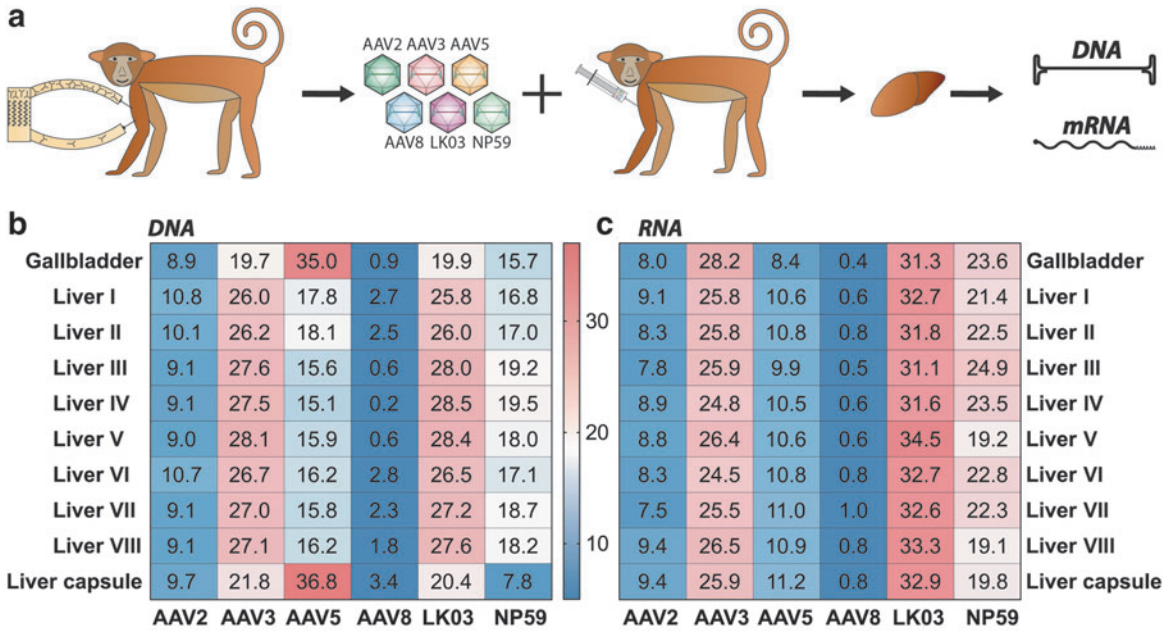

Figure 3. *In vivo* results cynomolgus monkey liver. **(a)** Schematic of column-based antibody depletion followed by NHP transduction. **(b)** NGS read contribution (%) for each AAV from whole tissue extracted DNA. **(c)** NGS read contribution (%) for each AAV from whole tissue mRNA-derived complementary DNA.

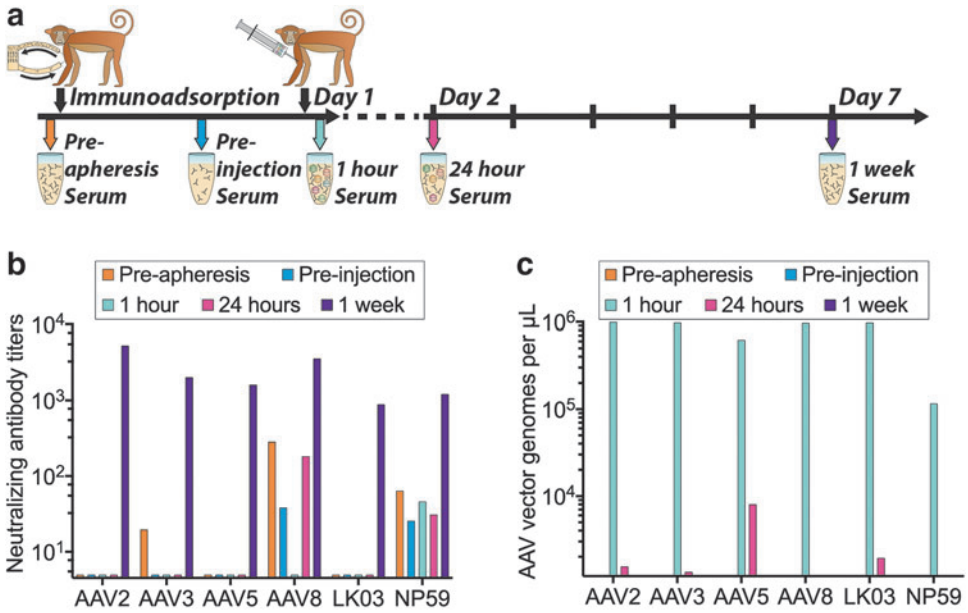

Figure 4. AAV-treated NHP serum analysis. **(a)** Schematic of serum collection before apheresis (antibody depletion), before AAV injection, 1 and 24 h after injection as well as at killing 1 week after injection. **(b)** NAb titers in collected serum at indicated time points for the indicated AAV variants. **(c)** AAV copy number per microliter and AAV variant from collected serum at indicated time points. NAb, neutralizing antibody.

est, AAV5 was the serotype that entered cells most efficiently in the gallbladder and liver capsule (Fig. 3b). AAV2 and AAV8 were the least efficient serotypes at cell entry (Fig. 3b). In terms of transgene expression, AAV-LK03 was the best performing variant, followed by AAV3b and AAV-NP59. AAV5, AAV2, and AAV8 performed relatively poorly (Fig. 3c). Although these observations require replication in additional NHPs, the hierarchies of capsid performance observed were sufficiently distinctive to offer preliminary insights worthy of discussion.

As the NHP experiment was terminated just 1 week after vector infusion, it is possible that expression from some of the AAV variants may not have reached the peak level.[58] It is therefore possible that AAVs that entered well (such as AAV5) could have, with time, led to higher mRNA expression compared with AAVs that entered less efficiently, but appear to have higher kinetics of expression (such as AAV-NP59). Although the authors appreciated the fact that the timing of the study could directly affect the study outcome, the main reason for the shorter timeline was to ensure consistency between *ex vivo* (1 week or less) and xenograft *in vivo* (1 week) experiments.

Based on previously published data, we were not surprised by the high performance of AAV-LK03.[55] It was also interesting to see how much better AAV-NP59 performed compared with the prototypical AAV2, which is highly homologous at the protein level, but potentially tissue culture adapted.[43] This indicates that the previously published advantage of lower HSPG binding could be beneficial in *in vivo* xenograft mouse models as well as NHP models.[31] As AAV-NP59 has not been evaluated in human studies, we can only rely on the hFRG, Rh/CyFRG and *in vivo* NHP data to infer clinical efficiency of this variant. Our data strongly suggest that AAV-NP59 would most likely perform substantially better than AAV2, but less efficiently than AAV3b/AAV-LK03, as we can see that the performance of AAV-NP59 in the CyFRG mice was overestimated compared with performance in Cynomolgus macaque *in vivo*. Finally, the most surprising finding from the NHP experiment was the very low AAV8 performance,[55] which warranted further investigation.

NHP serum analysis

Driven by the fact that AAV8 performance in the NHP liver was lower than anticipated based on published data,[55] we analyzed the levels of anti AAV NAbs in the serum harvested before AAV infusion. In addition, the clearance of AAVs from the serum was quantified. Both seroreactivity and AAV clearance were evaluated at five time points (Fig. 4a).

The NAb titers showed that the NHP had pre-existing NAbs against AAV3b, AAV8, and AAV-NP59 before apheresis. These NAb titers were reduced by the apheresis in all cases. Although the anti-AAV3 NAbs were effectively removed, antibodies against AAV8 and AAV-NP59 were not fully eliminated (Fig. 4b).

Seven days after vector administration we detected high NAb titers against all six AAV variants (Fig. 4b). Previous publications showed that even low NAb titers against AAV8 capsids could have a strong neutralization effect

in vivo in NHPs, and that this effect was substantially greater than expectations based on results from *in vitro* neutralization assays.[59,60] These published results lead us to the conclusion that the presence of residual anti-AAV8 NAbs can potentially explain, at least partially, the low performance of AAV8 vector *in vivo*.[47,59]

Although our data align well with published results, it is important to note that different methods of generating neutralization data can yield widely different results. This was highlighted by the comparison of *in vitro* and *in vivo*–generated NAb data published by Wang et al. in the case for AAV8.[60] The main reason for the divergence reported by the author was that AAVs transduce different cells with varying efficiencies (AAV2 is much better *in vitro* than *in vivo* compared with AAV8, and vice versa). Lower transduction efficiency means less sensitivity when evaluating antibody titers by neutralization and therefore every assay will be different depending on which doses and target cells are being used and whether adenoviral coinfection is used to boost transduction.[60]

With this in mind, we attempted to reduce experimental variability caused by varying transduction titers by establishing the required vector doses to achieve high transduction efficiency before the NAb assay for each of the AAVs. Although we understood that this approach does not address all the ambiguities of the neutralization assay, we hypothesize that it helped improve accuracy and thus the robustness of our data.

Analysis of AAV vector genomes in serum confirmed that substantial levels of AAV vectors were in circulation 1 h after the injection, and that most of the vectors were cleared within the first 24 h postinfusion. Particle concentrations were very similar between all variants apart from AAV-NP59, which showed an almost 10-fold lower concentration in the serum at the 1-h time point compared with all other variants (Fig. 4c), potentially indicating a faster uptake of AAV-NP59 by the liver, uptake by other tissues, or an uptake by certain immune cells owing to the observed interaction with NHP serum (Fig. 4b).

Effect of NHP serum on the transduction of AAV vectors in xenograft models of the human liver

Next, we wanted to take advantage of the humanized and ''simianized'' FRG models to investigate the potential impact of the anti-AAV NAbs in the NHP serum on vector transduction of primary hepatocytes. Using methods previously described,[40] the equimolar mix of AAVs was coincubated at a range of dilutions with NHP serum collected after the apheresis but before vector administration (Fig. 4a, ''preinjection serum''), and thus contained small titer of anti-AAV8 and anti-AAV-NP59 NAbs (Fig. 4b). The serum–AAV mix was subsequently injected into FRG mice repopulated with primary hepatocytes from either Rhesus macaque, Cynomolgus macaque, or human origin (Fig. 5a). Human and NHP hepatocytes, as well as murine hepatocytes, were recovered from livers harvested 7 days after systemic administration of the serum–AAV mix and individual vector transduction was analyzed at the DNA level using NGS of the barcoded genomic region.

AAV-NP59 was the top performer at the DNA level in FRG mice repopulated with Rhesus and Cynomolgus hepatocytes with and without vector preincubation with serum. However, the AAV-NP59 contribution in the group treated with the serum was substantially lower than that in the group transduced with untreated vectors (Fig. 5b), indicating that the anti-AAV-NP59 antibodies were partially neutralizing the vector and thus decreasing its performance. Of interest, there was no detected drop in the transduction efficiency of AAV8 following incubation with NHP sera. However, it is important to note that NGS percentages are relative to one another and thus the substantial drop in contribution from AAV-NP59 could mask a potentially reduced efficiency of neutralized AAV8. Indeed, relative transduction of all other vectors increased as the contribution of AAV-NP59 decreased, with AAV8 and AAV2 showing the lowest increase in transduction. This could indicate that the sera contained NAbs against those two variants.

Of interest, studies in FRG repopulated with human hepatocytes (hFRG) showed that performance of AAV-NP59 was not affected by the anti-AAV NAbs-containing serum and neither was the performance of AAV2, AAV3b, AAV5, or AAV-LK03, but the performance of AAV8 was reduced at the higher serum concentrations (Fig. 5b). All data shown as ''Rh/Cy/hFRG no sera'' are also used in Fig. 2b and are shown again for ease of comparability.

Finally, analysis of the mouse hepatocytes recovered from the chimeric livers showed a mild drop in the performance of AAV8 and AAV-NP59 for NHP and human-repopulated mice (Fig. 5c). Of interest, performance of AAV3b and AAV-LK03 in ''simianized'' FRGs appeared to have improved slightly following preincubation with NHP sera. Although this can be partially explained by the previously mentioned fact that NGS reads for each vector are relative to one another, the effect could also indicate an active interaction between AAV3-like capsids with components of the NHP serum, as similar findings for some AAVs have been reported for interactions with human sera in mice.[61] It is also important to note that the immunodeficient FRG mouse model may not fully recapitulate what happens to AAV–antibody complexes in immunocompetent NHPs *in vivo*, as many immune cells are not fully developed.

Seroprevalence of NAbs against capsids used in this study

As transduction efficiency of an AAV capsid can be negatively affected by NAbs, pre-existing immunity can exclude patients from an AAV gene therapy trial or clinical treatment.[62] Therefore, we assessed the seroprevalence of NAbs against AAV variants used in this

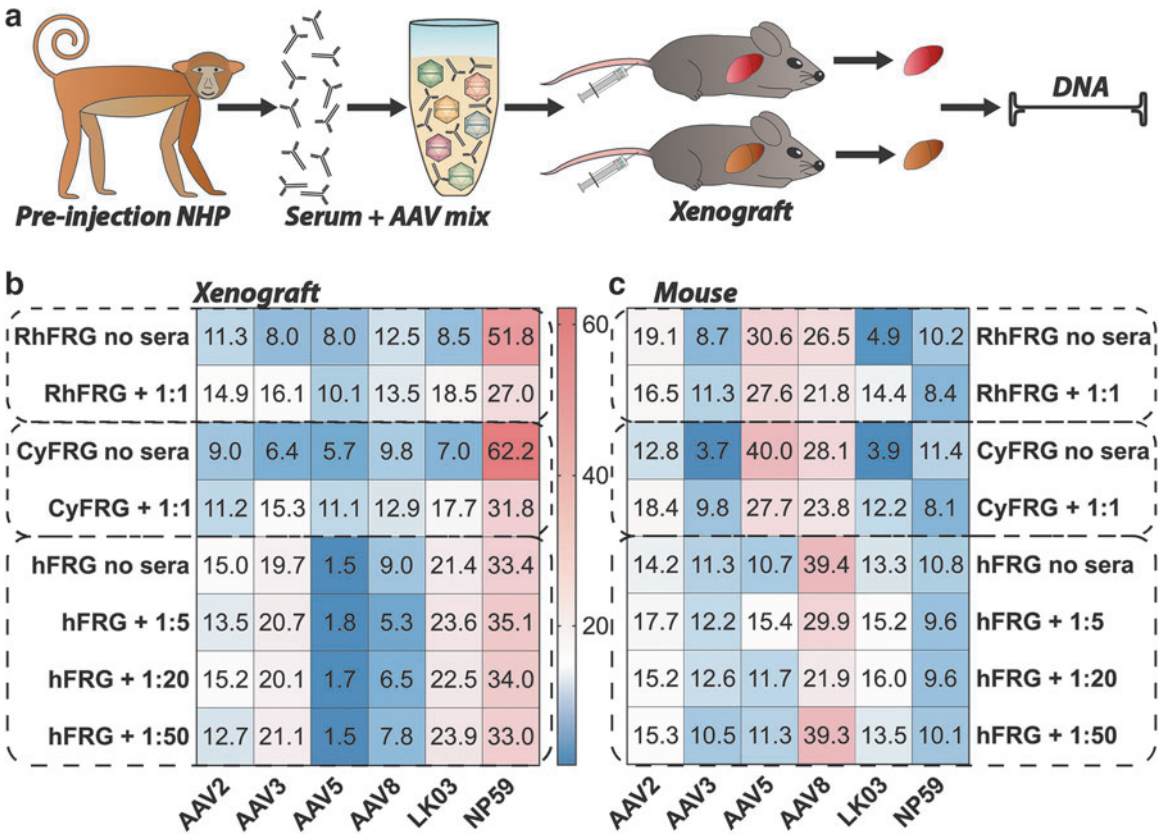

Figure 5. *In vivo* transduction with NHP preinjection serum-incubated AAV mix. **(a)** Schematic of transduction of engrafted FRG mice with coincubated AAV mix and antibodies from the postapheresis/preinjection step of the experiment using *Macaca fascicularis* NHP. **(b)** NGS read contribution (%) for each AAV from extracted xenograft DNA in absence or presence of serum in indicated dilutions. Cells were sorted for xenograft species. **(c)** NGS read contribution (%) for each AAV from mouse extracted DNA in absence or presence of serum in indicated dilutions. Cells were sorted for mouse origin. All data shown as "Rh/Cy/hFRG no sera" are also used for Fig. 2b and are shown again for ease of comparability. hFRG, humanized FRG.

study in 85 human samples. Samples were collected from individuals younger than 1-year old (17%), aged 1–5 years (35%), 6–10 years (16%), 11–20 years (12%), and older than 20 years (20%). The overall seroprevalence of NAb ranged from 14% (AAV5) to 29% (AAV3b) (Fig. 6a).

Seroprevalence was low during the first years of age and increased after the age of 10 years (Fig. 6b). NAb titers are higher for AAV3b, AAV2, and AAV-NP59 with median of 1/320, 1/160 and 1/80, respectively. Lower NAb titers were observed for AAV5, AAV8, and AAV-LK03 with medians of 1/5, 1/5 and 1/20, respectively (Fig. 6c). Strong cross-reactivity with other liver-tropic capsids tested was detected for AAV2, AAV-NP59, and AAV5 (Fig. 6d).

In the cohort of plasma samples tested for seroprevalence, 80% were from persons aged 20 years or younger. This work corroborates previous findings that most pediatric individuals have not yet developed anti-AAV antibodies, which emphasizes a decisive immunological advantage of targeting this age group.[63,64] The seroprevalence rates increased rapidly in teenage and adulthood where NAb seroprevalence rates could be as high as 80% for the some AAV serotypes.[27,64–68] Our data for sera from the adult population showed lower neutralization rates compared with other seroprevalence studies[66] but the findings were in accordance with our previous work in the British population.[46] AAV2, AAV3b, and surprisingly AAV-NP59 showed higher titers compared with AAV5, AAV8, and AAV-LK03, although the use of a higher dose for AAV5 and AAV8 may have reduced the sensitivity and partly underestimated the titers.[69]

NAb cross-reactivity was high between some liver-tropic capsids.[46,64,66] These findings support the need for innovative immunosuppression protocols or antibody reduction methods to allow successful transduction in pre-immunized patients and readministration, if needed.[62] Antibody reduction has previously been performed either by removing all antibodies (as has been used for the NHP in the presented study)[47] or by specifically removing anti-AAV antibodies.[70,71] Another recently reported option is to use IgG degrading enzymes, which would be infused systemically before AAV delivery.[72,73] These methods would be especially relevant for use in infants, who are only passively immunized through adoptive transfer from the mother and do not have memory cells specific against AAV epitopes, making it less likely for their immune system to be activated.

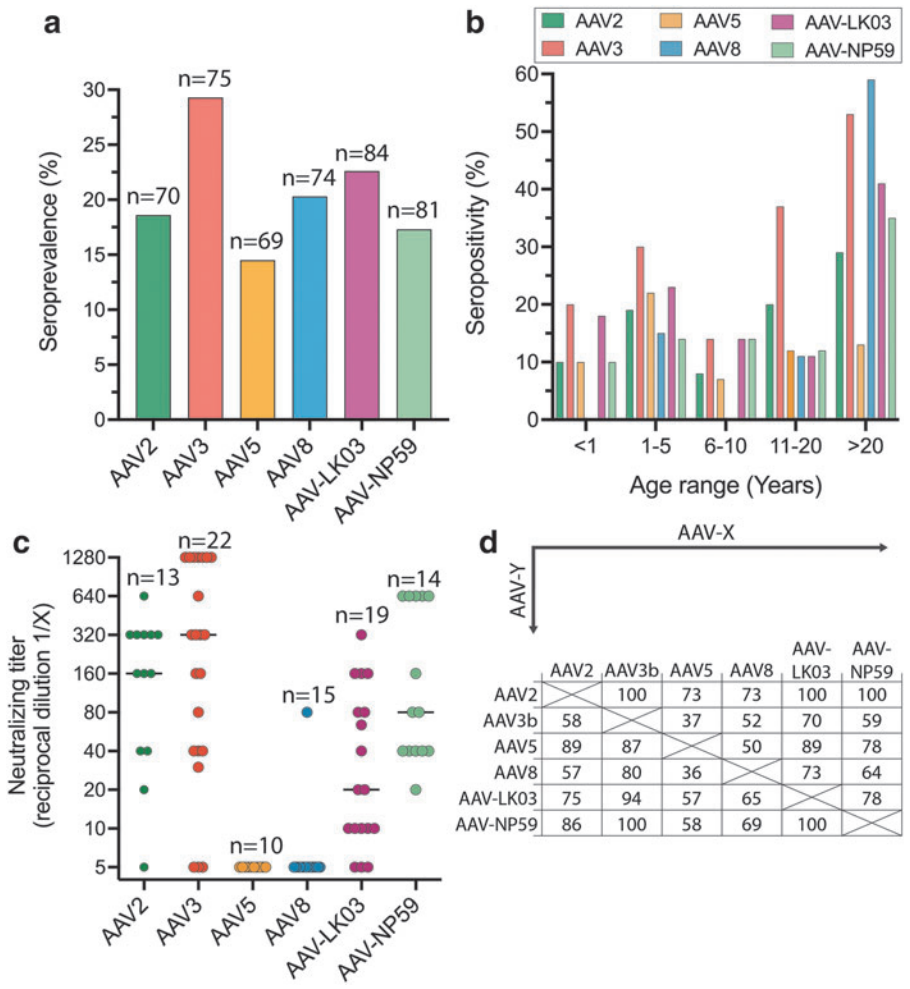

Figure 6. Seroprevalence and titers of NAbs of liver-tropic capsids. **(a)** Seroprevalence per AAV serotype. **(b)** Seroprevalence according to age. **(c)** Neutralizing titer per serotype. Each *dot* represents a seropositive sample. The *line* represents the median. **(d)** Cross-reactivity by AAV serotype. Shown are the percentage of samples that are positive for AAV-X in samples that were positive for AAV-Y.

CONCLUSIONS

Expectedly, we observed that the interaction of the AAV vectors and the target hepatocytes differed in *in vitro* and *ex vivo* cells as well as xenograft models and *in vivo* NHP transductions, recognizing the potential limitation of our conclusions arising from using only a single NHP in our study. However, although a perfectly predictive preclinical model does not exist, our study shows that each model provides a unique insight into the vector function. Yet, without the benefit of clinical data, where each of the vectors would be tested for the delivery of the same transgene cassette to the liver, it is impossible to determine, with a high level of certainty, which of the models is the most predictive of human outcome.

Based on our results and the fact that each model brings a unique perspective that adds to the overall functional evaluation of AAV vectors, we propose that multiple models should be used to paint a more complete picture and help us make the most informed decision as to which vector should be used in each clinical application. To do so, it is critical to understand the strengths and weaknesses of each model. Specifically, our data confirmed that many tissue culture models are overly dependent on strong AAV binding to HSPG, which may not be directly applicable to an *in vivo* setting.[31,43]

We also found that AAV5 generally performed better in primary NHP hepatocytes *ex* and *in vivo* compared with human hepatocytes in the same experimental settings. As this finding was consistent between models, it may explain the lower-than-expected outcomes in several clinical trials using AAV5 to target the human liver.[24,25] As AAV8 performed better in NHP-FRGs than in hFRGs, our data could suggest that a similar mechanism could affect AAV8's performance in human hepatocytes.

In general, our study showed that the FRG mouse model offers high flexibility and utility as it can be repopulated with primary hepatocytes from human and NHPs.[74] Thus, this xenograft model allows investigators to gain a unique insight into the cross-species transferability of the AAV performances data from NHPs, the most sought after

preclinical model of human liver, to human patients. Furthermore, our data showed that the correlation between data obtained from NHP and xenograft model was not perfect. This could be owing to complex, and not fully understood, interactions between xenograft and mouse hepatocytes, competition in AAV uptake between the species, or the absence of a complete immune system in the mice. One conclusion that becomes apparent from our study was that compared with the NHP data, the NHP hepatocytes in the FRG mouse appear to have an increased uptake of AAV-NP59 and a reduced uptake of AAV5.

However, the NHP model may not be perfect either. Apart from ethical considerations around the use of NHPs in biomedical research, availability and cost can be prohibitive. The cost and availability of NHPs is also affected by the fact that animals need to be screened for pre-existing anti-AAV NAbs. Finally, the fact that wild-type, outbred NHPs are used, leads to the requirement of using higher number of animals per group to account for natural differences between ''subjects.''

Based on the data presented, our current understanding of the individual preclinical models, as well as our insights into the AAV–cell interactions, we propose that initial studies of liver-targeting AAVs should include hFRG mice in the presence of human serum and/or pooled IgG before initiating studies involving large animals.

It is, however, critical to note that all models used in this study have a number of critical limitations that could not have been addressed in this article. For example, no model system was yet found to fully recapitulate the anti-AAV cellular immune responses seen in clinical trials.[13,14] Although the immune-deficient FRG mice are not the most suitable model to test immune responses to transduction, a hybrid xenograft FRG mouse containing the hematopoietic system and the hepatocytes from matching human donors might be a possibility in the future.

Based on data from a hemophilia A clinical trial for AAV-LK03[30] as well as data from this study (good efficiency at transducing NHP and human hepatocytes *ex vivo* and *in vivo* in the xenograft model and the NHP, and relatively low pre-existing immunity in the general population), we anticipate that the next-generation bioengineered AAV-LK03 and AAV-NP59 vectors will be strong clinical candidates for liver targeted therapies.

AUTHORS' CONTRIBUTIONS

A.W., M.C.-C., E.Z., D.S.G., D.P.P., S.A.W., J.B., G.G-A., and L.L. designed the experiments. A.W., M.C-C., K.L.D., E.Z., D.S.G., R.G.N., S.S., M.K., A.M., S.F., D.P.P., B.M.T., E.V., S.L.W., S.A.W., and L.L. generated reagents, protocols, performed experiments, and analyzed data. A.W., A.K.A., and L.L. wrote the article and generated the figures. All authors reviewed, edited, and commented on the article.

DISCLAIMER

The views expressed are those of the author(s) and not necessarily those of the NHS, the NIHR or the Department of Health.

AUTHOR DISCLOSURE

L.L., I.E.A. and A.J.T. have commercial affiliations. L.L. and I.A.E. have consulted on technologies discussed in this article. L.L. and I.A.E. have stock and/or equity in companies with technologies broadly related to this study. L.L. is a co-inventor of, and receives licensing royalties from, several AAV variants used in the study. A.L.M. and T.E.H. are employees, shareholders, and/or optionees of Inventia Life Science Pty. Ltd. Inventia has an interest in commercializing the 3D bioprinting technology. All other authors declare no competing financial interests.

FUNDING INFORMATION

This work was supported by project grants from the Australian National Health and Medical Research Council (NHMRC) to L.L. and I.E.A. (APP1108311, APP1156431 and APP1161583) and Paediatrio Paediatric Precision Medicine Program to L.L. (PPM1K5116/RD274). Work presented in Figs. 3 and 4 were supported by funding from LogicBio Therapeutics. L.L. was also supported by research grants from the Department of Science and Higher Education of Ministry of National Defense, Republic of Poland, (''Kościuszko'' k/10/8047/DNiSW/T—WIHE/3) and from the National Science Centre, Republic of Poland (OPUS 13) (UMO-2017/25/B/NZ1/02790).

The work of I.E.A. was also supported by an Australian Research Council (ARC) Discovery Project (DP150101253). A.J.T. was supported by funding from The Wellcome Trust (Grant No. 217112/Z/19/Z AJT). This work was supported by funding to J.B. from the NIHR Great Ormond Street Hospital Biomedical Research Centre; Medical Research Council Grant/Award Number: MR/T008024/1; National Institute for Health Research; Innovate UK Biomedical Catalyst Early stage award 14720; Nutricia Metabolic Research Grant; London Advanced Therapy/Confidence in Collaboration award 2CiC017.

SUPPLEMENTARY MATERIAL

Supplementary Figure S1
Supplementary Figure S2
Supplementary Figure S2
Supplementary Figure S4
Supplementary Table S1
Supplementary Table S2
Supplementary Table S3

REFERENCES

1. Hoggan MD, Blacklow NR, Rowe WP. Studies of small DNA viruses found in various adenovirus preparations: physical, biological, and immunological characteristics. Proc Natl Acad Sci 1966; 55(6):1467.
2. Srivastava A, Lusby EW, Berns KI. Nucleotide sequence and organization of the adeno-associated virus 2 genome. J Virol 1983;45(2): 555–564.
3. Samulski RJ, Berns KI, Tan M, et al. Cloning of adeno-associated virus into pBR322: Rescue of intact virus from the recombinant plasmid in human cells. Proc Natl Acad Sci 1982;79(6):2077–2081.
4. Samulski RJ, Muzyczka N. AAV-mediated gene therapy for research and therapeutic purposes. Annu Rev Virol 2014;1(1):427–451.
5. Grimm D, Pandey K, Nakai H, et al. Liver transduction with recombinant adeno-associated virus is primarily restricted by capsid serotype not vector genotype. J Virol 2006;80(1):426–439.
6. Wu Z, Asokan A, Samulski RJ. Adeno-associated virus serotypes: Vector Toolkit for human gene therapy. Mol Ther 2006;14(3):316–327.
7. Russell S, Bennett J, Wellman JA, et al. Efficacy and safety of voretigene neparvovec (AAV2-hRPE65v2) in patients with RPE65-mediated inherited retinal dystrophy: A randomised, controlled, open-label, phase 3 trial. Lancet 2017;390(10097): 849–860.
8. Mendell JR, Al-Zaidy S, Shell R, et al. Single-dose gene-replacement therapy for spinal muscular atrophy. N Engl J Med 2017; 377(18):1713–1722.
9. Gaudet D, Méthot J, Déry S, et al. Efficacy and long-term safety of alipogene tiparvovec (AAV1-LPLS447X) gene therapy for lipoprotein lipase deficiency: An open-label trial. Gene Ther 2013; 20(4):361–369.
10. Dunbar CE, High KA, Joung JK, et al. Gene therapy comes of age. Science 2018;359(6372): eaan4672.
11. Maestro S, Weber ND, Zabaleta N, et al. Novel vectors and approaches for gene therapy in liver diseases. JHEP Rep 2021;3(4).
12. Verdera HC, Kuranda K, Mingozzi F. AAV vector immunogenicity in humans: A long journey to successful gene transfer. Mol Ther 2020;28(3): 723–746.
13. Manno CS, Pierce GF, Arruda VR, et al. Successful transduction of liver in hemophilia by AAV-Factor IX and limitations imposed by the host immune response. Nat Med 2006;12(3):342–347.
14. Mingozzi F, Maus MV, Hui DJ, et al. CD8+ T-cell responses to adeno-associated virus capsid in humans. Nat Med 2007;13(4):419–422.
15. Mount JD, Herzog RW, Tillson DM, et al. Sustained phenotypic correction of hemophilia B dogs with a factor IX null mutation by liver-directed gene therapy. Blood 2002;99(8):2670–2676.
16. George LA, Ragni MV, Rasko JEJ, et al. Long-term follow-up of the first in human intravascular delivery of AAV for gene transfer: AAV2-hFIX16 for severe hemophilia B. Mol Ther 2020;28(9):2073–2082.
17. Gao GP, Alvira MR, Wang L, et al. Novel adeno-associated viruses from rhesus monkeys as vectors for human gene therapy. Proc Natl Acad Sci 2002;99(18):11854.
18. Bantel-Schaal U, zur Hausen H. Characterization of the DNA of a defective human parvovirus isolated from a genital site. Virology 1984;134(1): 52–63.
19. Davidoff AM, Gray JT, Ng CY, et al. Comparison of the ability of adeno-associated viral vectors pseudotyped with serotype 2, 5, and 8 capsid proteins to mediate efficient transduction of the liver in murine and nonhuman primate models. Mol Ther 2005;11(6):875–888.
20. Nathwani AC, Gray JT, McIntosh J, et al. Safe and efficient transduction of the liver after peripheral vein infusion of self-complementary AAV vector results in stable therapeutic expression of human FIX in nonhuman primates. Blood 2006; 109(4):1414–1421.
21. Nathwani AC, Tuddenham EG, Rangarajan S, et al. Adenovirus-associated virus vector–mediated gene transfer in hemophilia B. N Engl J Med 2011; 365(25):2357–2365.
22. Nathwani AC, Reiss UM, Tuddenham EG, et al. Long-term safety and efficacy of factor IX gene therapy in hemophilia B. N Engl J Med 2014; 371(21):1994–2004.
23. Majowicz A, Nijmeijer B, Lampen MH, et al. Therapeutic hFIX activity achieved after single AAV5-hFIX treatment in hemophilia B patients and NHPs with pre-existing anti-AAV5 NABs. Mol Ther Methods Clin Dev 2019;14:27–36.
24. Miesbach W, Meijer K, Coppens M, et al. Gene therapy with adeno-associated virus vector 5–human factor IX in adults with hemophilia B. Blood 2018;131(9):1022–1031.
25. Von Drygalski A, Giermasz A, Castaman G, et al. Etranacogene dezaparvovec (AMT-061 phase 2b): Normal/near normal FIX activity and bleed cessation in hemophilia B. Blood Adv 2019;3(21): 3241–3247.
26. Lisowski L, Dane AP, Chu K, et al. Selection and evaluation of clinically relevant AAV variants in a xenograft liver model. Nature 2014;506:382.
27. Paulk NK, Pekrun K, Zhu E, et al. Bioengineered AAV capsids with combined high human liver transduction in vivo and unique humoral seroreactivity. Mol Ther 2018;26(1):289–303.
28. Azuma H, Paulk N, Ranade A, et al. Robust expansion of human hepatocytes in Fah–/–/Rag2–/–/Il2rg–/– mice. Nat Biotechnol 2007; 25(8):903–910.
29. Rutledge EA, Halbert CL, Russell DW. Infectious clones and vectors derived from adeno-associated virus (AAV) serotypes other than AAV type 2. J Virol 1998;72(1):309–319.
30. George LA, Monahan PE, Eyster ME, et al. Multiyear factor VIII expression after AAV gene transfer for hemophilia A. N Engl J Med 2021; 385(21):1961–1973.
31. Cabanes-Creus M, Westhaus A, Navarro RG, et al. Attenuation of heparan sulfate proteoglycan binding enhances in vivo transduction of human primary hepatocytes with AAV2. Mol Ther Methods Clin Dev 2020;17:1139–1154.
32. Gonzalez TJ, Simon KE, Blondel LO, et al. Cross-species evolution of a highly potent AAV variant for therapeutic gene transfer and genome editing. Nat Commun 2022;13(1):5947.
33. Au HKE, Isalan M, Mielcarek M. Gene therapy advances: A meta-analysis of AAV usage in clinical settings. Front Med (Lausanne) 2022;8: 809118.
34. Adachi K, Enoki T, Kawano Y, et al. Drawing a high-resolution functional map of adeno-associated virus capsid by massively parallel sequencing. Nat Commun 2014;5:3075.
35. Weinmann J, Weis S, Sippel J, et al. Identification of a myotropic AAV by massively parallel in vivo evaluation of barcoded capsid variants. Nat Commun 2020;11(1):5432.
36. Westhaus A, Cabanes-Creus M, Rybicki A, et al. High-throughput in vitro, ex vivo, and in vivo screen of adeno-associated virus vectors based on physical and functional transduction. Hum Gene Ther 2020;31(9–10):575–589.
37. Westhaus A, Cabanes-Creus M, Jonker T, et al. AAV-p40 bioengineering platform for variant selection based on transgene expression. Hum Gene Ther 2022;33(11–12):664–682.
38. Utama RH, Atapattu L, O'Mahony AP, et al. A 3D bioprinter specifically designed for the high-throughput production of matrix-embedded multicellular spheroids. iScience 2020;23(10):101621.
39. Jung MS, Skhinas JN, Du EY, et al. A high-throughput 3D bioprinted cancer cell migration and invasion model with versatile and broad biological applicability. bioRxiv 2021; doi: 10.1101/2021.12.28.474387
40. Cabanes-Creus M, Navarro RG, Zhu E, et al. Novel human liver-tropic AAV variants define transferable domains that markedly enhance the human tropism of AAV7 and AAV8. Mol Ther Methods Clin Dev 2022;24:88–101.
41. Flanagan DJ, Schwab RHM, Tran BM, et al. Isolation and Culture of Adult Intestinal, Gastric, and Liver Organoids for Cre-Recombinase-Mediated Gene Deletion. In: Organoids: Stem Cells, Struc-

ture, and Function. Methods in Molecular Biology (Turksen K, ed.) Humana Press: New York, NY, USA; 2019; Vol. 1576; pp. 123–133.

42. Wei J, Ran G, Wang X, et al. Gene manipulation in liver ductal organoids by optimized recombinant adeno-associated virus vectors. J Biol Chem 2019; 294(38):14096–14104.

43. Cabanes-Creus M, Hallwirth CV, Westhaus A, et al. Restoring the natural tropism of AAV2 vectors for human liver. Sci Transl Med 2020; 12(560):eaba3312.

44. Cabanes-Creus M, Navarro RG, Liao SHY, et al. Single amino acid insertion allows functional transduction of murine hepatocytes with human liver tropic AAV capsids. Mol Ther Methods Clin Dev 2021;21:607–620.

45. Cabanes-Creus M, Ginn SL, Amaya AK, et al. Codon-optimization of wild-type adeno-associated virus capsid sequences enhances DNA family shuffling while conserving functionality. Mol Ther Methods Clin Dev 2019;12:71–84.

46. Perocheau DP, Cunningham S, Lee J, et al. Age-related seroprevalence of antibodies against AAV-LK03 in a UK Population Cohort. Hum Gene Ther 2018;30(1):79–87.

47. Salas D, Kwikkers KL, Zabaleta N, et al. Immunoadsorption enables successful rAAV5-mediated repeated hepatic gene delivery in nonhuman primates. Blood Adv 2019;3(17):2632–2641.

48. Nakabayashi H, Taketa K, Miyano K, et al. Growth of human hepatoma cell lines with differentiated functions in chemically defined medium. Cancer Res 1982;42(9):3858.

49. López-Terrada D, Cheung SW, Finegold MJ, et al. Hep G2 is a hepatoblastoma-derived cell line. Hum Pathol 2009;40(10):1512–1515.

50. Prior N, Inacio P, Huch M. Liver organoids: From basic research to therapeutic applications. Gut 2019;68(12):2228.

51. Belfiore L, Aghaei B, Law AMK, et al. Generation and analysis of 3D cell culture models for drug discovery. Eur J Pharm Sci 2021;163: 105876.

52. Xiong T, Li J, Chen F, et al. PCAT-1: A novel oncogenic long non-coding RNA in human cancers. Int J Biol Sci 2019;15(4):847–856.

53. Yang Z, Zhao S, Zhou X, et al. PCAT-1: A pivotal oncogenic long non-coding RNA in human cancers. Biomed Pharmacother 2019;110:493–499.

54. Paine-Saunders S, Viviano BL, Saunders S. GPC6, a novel member of the glypican gene family, encodes a product structurally related to GPC4 and is colocalized with GPC5 on human chromosome 13. Genomics 1999;57(3):455–458.

55. Wang L, Bell P, Somanathan S, et al. Comparative study of liver gene transfer with AAV vectors based on natural and engineered AAV capsids. Mol Ther 2015;23(12):1877–1887.

56. Monaci P, Nicosia A, Cortese R, et al. Two different liver-specific factors stimulate in vitro transcription from the human alpha 1-antitrypsin promoter. EMBO J 1988;7(7):2075–2087.

57. Simonet WS, Bucay N, Lauer SJ, et al. A far-downstream hepatocyte-specific control region directs expression of the linked human apolipoprotein E and C-I genes in transgenic mice. J Biol Chem 1993;268(11):8221–8229.

58. Thomas CE, Storm TA, Huang Z, et al. Rapid uncoating of vector genomes is the key to efficient liver transduction with pseudotyped adeno-associated virus vectors. J Virol 2004;78(6):3110.

59. Wang L, Calcedo R, Wang H, et al. The pleiotropic effects of natural AAV infections on liver-directed gene transfer in macaques. Mol Ther 2010;18(1): 126–134.

60. Wang L, Calcedo R, Bell P. Impact of pre-existing immunity on gene transfer to nonhuman primate liver with adeno-associated virus 8 vectors. Hum Gene Ther 2011;22(11):1389–1401.

61. Wang M, Sun J, Crosby A, et al. Direct interaction of human serum proteins with AAV virions to enhance AAV transduction: Immediate impact on clinical applications. Gene Ther 2017;24(1):49–59.

62. Weber T. Anti-AAV antibodies in AAV gene therapy: Current challenges and possible solutions. Front Immunol 2021;12:658399.

63. Calcedo R, Morizono H, Wang L, et al. Adeno-associated virus antibody profiles in newborns, children, and adolescents. Clin Vaccine Immunol 2011;18(9):1586–1588.

64. Li C, Narkbunnam N, Samulski RJ, et al. Neutralizing antibodies against adeno-associated virus examined prospectively in pediatric patients with hemophilia. Gene Ther 2012;19(3):288–294.

65. Baruteau J, Waddington SN, Alexander IE, et al. Gene therapy for monogenic liver diseases: Clinical successes, current challenges and future prospects. J Inherit Metab Dis 2017;40(4):497–517.

66. Boutin S, Monteilhet V, Veron P, et al. Prevalence of serum IgG and neutralizing factors against adeno-associated virus (AAV) types 1, 2, 5, 6, 8, and 9 in the healthy population: Implications for gene therapy using AAV vectors. Hum Gene Ther 2010;21(6):704–712.

67. Ling C, Wang Y, Feng YL, et al. Prevalence of neutralizing antibodies against liver-tropic adeno-associated virus serotype vectors in 100 healthy Chinese and its potential relation to body constitutions. J Integr Med 2015;13(5):341–346.

68. Louis Jeune V, Joergensen JA, Hajjar RJ, et al. Pre-existing anti–adeno-associated virus antibodies as a challenge in AAV gene therapy. Hum Gene Ther Methods 2013;24(2):59–67.

69. Meliani A, Leborgne C, Triffault S, et al. Determination of anti-adeno-associated virus vector neutralizing antibody titer with an In Vitro Reporter System. Hum Gene Ther Methods 2015;26(2):45–53.

70. Bertin B, Veron P, Leborgne C, et al. Capsid-specific removal of circulating antibodies to adeno-associated virus vectors. Sci Rep 2020;10(1):864.

71. Orlowski A, Katz MG, Gubara SM, et al. Successful transduction with AAV Vectors after selective depletion of anti-AAV antibodies by immunoadsorption. Mol Ther Methods Clin Dev 2020;16:192–203.

72. Elmore ZC, Oh DK, Simon KE, et al. Rescuing AAV gene transfer from neutralizing antibodies with an IgG-degrading enzyme. JCI Insight 2020;5(19): e139881.

73. Leborgne C, Barbon E, Alexander JM, et al. IgG-cleaving endopeptidase enables in vivo gene therapy in the presence of anti-AAV neutralizing antibodies. Nat Med 2020;26(7):1096–1101.

74. Hatit MZC, Lokugamage MP, Dobrowolski CN, et al. Species-dependent in vivo mRNA delivery and cellular responses to nanoparticles. Nat Nanotechnol 2022;17(3):310–318.

Received for publication October 1, 2022;
accepted after revision February 19, 2023.

Published online: March 16, 2023.